Electronic Structure of Warm Dense Copper Studied by Ultrafast X-Ray Absorption Spectroscopy

B. I. Cho, K. Engelhorn, A. A. Correa, T. Ogitsu, C. P. Weber, H. J. Lee, J. Feng, P. A. Ni, Y. Ping, A. J. Nelson, D. Prendergast, R. W. Lee, R. W. Falcone, and P. A. Heimann

Phys. Rev. Lett. **106**, 167601 — Published 20 April 2011

DOI: 10.1103/PhysRevLett.106.167601

Electronic Structure of Warm Dense Copper Studied by Ultrafast X-ray Absorption Spectroscopy

B. I. Cho,[1] K. Engelhorn,[1] A. A. Correa,[2] T. Ogitsu,[2] C. P. Weber,[3] H. J. Lee,[4] J. Feng,[1]

P. A. Ni,[5] Y. Ping,[2] A. J. Nelson,[2] D. Prendergast,[6] R. W. Lee,[2] R. W. Falcone[1,7] and

P. A. Heimann[1]

[1]*Advanced Light Source, Lawrence Berkeley National Laboratory, Berkeley, CA 94720*

[2]*Lawrence Livermore National Laboratory, Livermore, CA 94550*

[3]*Department of Physics, Santa Clara University, Santa Clara, CA 95053*

[4]*Linac Coherent Light Source, SLAC National Accelerator Laboratory, Menlo Park, CA 94025*

[5]*Accelerator and Fusion Research, Lawrence Berkeley National Laboratory, Berkeley, CA 94720*

[6]*Molecular Foundry, Lawrence Berkeley National Laboratory, Berkeley, CA 94720*

[7]*Department of Physics, University of California, Berkeley, CA 94720*

Abstract

We use time-resolved x-ray absorption spectroscopy to investigate the unoccupied electronic density of states of warm dense copper that is produced isochorically through the absorption of an ultrafast optical pulse. The temperature of the superheated electron-hole plasma, which ranges from 4000 to 10000 K, was determined by comparing the measured x-ray absorption spectrum with a simulation. The electronic structure of warm dense copper is adequately described with the high temperature electronic density of state calculated by the density functional theory. The dynamics of the electron temperature are consistent with a two-temperature model, while a temperature-dependent electron-phonon coupling parameter is necessary.

Understanding the properties of warm dense matter (WDM) is a research area that has attracted much interest recently [1-4]. The WDM regime falls in between condensed matter and plasmas, where it is defined by temperatures of ~ 10^4-10^5 K (~ 1-10 eV) and near solid densities [5]. The theoretical description of WDM is quite different from both traditional plasma and/or condensed matter physics, because the thermal energy is comparable the Fermi energy and the ion-ion coupling parameter is of order unity. Nonetheless, studying this superheated solid or strongly coupled plasma can provide key understandings about non-equilibrium phase transitions and energy relaxation processes, which are critical to model many phenomena found in astrophysics [6], inertial confinement fusion [7], as well as the applied processes of laser machining and ablation [8].

For quantitative WDM studies one should determine the physical quantities, such as density, pressure and temperature. By using a femtosecond laser, isochoric heating of the sample with a known density is obtained [1, 2]. On the other hand, measurement of temperature has proven to be difficult. For temperature, optical pyrometry has low signal level for ultrafast measurements, and accurate temperature determination is limited by uncertainty in the emissivity for the WDM regime [9]. Although x-ray Thomson scattering has demonstrated the capability to determine the temperature in addition to the electron density and ionization degree [3], at present Thomson scattering has a temperature uncertainty that will be relatively large for these low temperatures, ~ 1eV.

As WDM states are predominantly non-equilibrium, ultrafast techniques are essential to probe the transient (~ ps) material properties. In this way the optical properties of warm dense gold have been successfully investigated [1]. However, because of the near solid density of WDM, the probing depth with optical lasers is limited. On the other hand, x-ray absorption

spectroscopy provides information on electronic structure and optical pump / x-ray probe techniques have been developed to study dynamical properties [10]. Recently, a study of the x-ray absorption spectrum (XAS) of warm dense aluminum heated by laser-accelerated protons was reported [4]. A broadening of the *K* edge was observed that was caused by the change in the electron distribution associated with the high temperature. In addition, they interpreted a loss of structure in the XAS as resulting from a loss of order in the high temperature liquid. For Cu, a photoemission study using ultrafast laser-heating observed a reduced intensity in the *3d* peak. This change was interpreted as caused by a lower occupation of the *d* band at the elevated electron temperature [2].

Here we present a study of the electronic structure of warm dense copper created by ultrafast laser excitation and probed by time resolved x-ray absorption spectroscopy. Under strong optical excitation, the electron temperature T_e of solid density Cu is quickly increased to ~ 1 eV. The experimental XAS was compared with the theoretical one derived from first-principles Density Functional Theory (DFT) simulations. The time dependence of T_e determined from XAS allows us to study the electron-phonon coupling of the non-equilibrium state of warm dense copper.

The experiment was performed at beamline 6.0.2 of the Advanced Light Source (ALS) synchrotron radiation facility. The laser pump and x-ray probe setup is depicted in Fig 1. A Ti:sapphire laser pulse with duration of 150 fs is split into three paths. The first pulse is frequency doubled and focused (250 × 200 μm FWHM) onto the foil to isochorically heat the Cu sample. The second pulse triggers the x-ray streak camera. The third is frequency tripled and split to generate two timing fiducials imaged along with an x-ray pulse. The sample is composed of a freestanding Cu foil of 70 nm thickness coated on both sides with 6 nm of amorphous

carbon to prevent oxidation of the Cu. A measurement of the reflection and transmission of the 400 nm laser light indicates that 60% of the laser energy is absorbed in the sample. The experiments are performed at the laser fluence (0.33 ± 0.07 J/cm^2) above the damage threshold, therefore the sample is translated to a fresh location after each laser shot.

The probe is provided by broadband, 70 ps pulse duration x-rays from an ALS undulator tuned to the Cu *L* edges. The x-ray bandwidth and the imaging of the streak camera allow the entire X-ray Absorption Near-Edge Structure (XANES) to be detected for each x-ray pulse. The x-ray spot size was set to 200×150 μm for the spatial overlap with the laser focus. X-rays transmitted through the sample enter a Variable-Line-Spacing (VLS) grating spectrometer, which provides an energy resolution of 1.1 eV at the Cu *L* edges [11]. Dispersed x-rays enter the streak camera, which has a temporal resolution of 2 ps. This streak camera detector provides 2-dimensional images of the x-ray pulse with time on one axis and photon energy on the other [12].

The optical photons are absorbed by the 3*d*-4*p* interband transition. This absorption process occurs near the front surface of the sample because of the 14 nm optical penetration depth in Cu. However, the ballistic motion of excited electrons delivers energy through the depth of the sample since the sample thickness is set to the mean free path of electrons in solid Cu, 70 nm [13]. Fourier Domain Interferometry (FDI) of Cu indicates a surface expansion velocity of ~ 1 nm/ps therefore a near-constant density will be maintained for a time of order a few ps following the ultrafast laser pulse [14].

Fig. 2 exhibits the XAS of warm dense copper at selected times which are obtained from an average of 150 streak camera images. At the streak camera the x-ray intensity is estimated to be 10^4 (pulse eV 2 ps)$^{-1}$. The initially deposited energy density is $3.6 \pm 0.7 \times 10^6$ J/kg. The room temperature spectrum is observed without a laser pulse and is averaged over 70 ps. The three

peaks of XANES spectrum follow the observed solid Cu spectrum under ambient conditions [15]. Because of the 2 ps streak camera time resolution, the XAS at $t = 0$ includes an average of the WDM spectra and the room temperature spectrum. At 2 ps, the position of the L_3 edge is shifted to lower photon energy, and the absorption above the original L_3 edge is decreased. Around the L_2 edge, the same phenomena are observed although the effects are smaller because of the larger L_2 natural linewidth caused by the allowed Coster-Kronig Auger transition. After 6 ps, the L_3 edge appears broadened, and by 20 ps time delay the difference from the room temperature XAS is further reduced. These dynamics indicate that electrons are excited from below to above the Fermi level E_F, and that there is a relaxation of the electronic excitation on a time scale of ~ 6 ps.

To further interpret the measured XAS, it is necessary to compare with simulations. At high temperatures, liquid atomic configurations are generated using first-principles Density Functional Theory (DFT) molecular dynamics (MD) simulations. For the initial state, a face centered cubic solid at ambient conditions is assumed. For the state following the laser pulse, liquid atomic configurations at electron temperature, T_e of 12448 K and ion temperature, T_i of 3846 K are used. A constant density of solid copper is used for the calculations. It should be noted that the calculated x-ray absorption cross section was not very sensitive to the T_e and T_i used for the MD simulations. Therefore, T_e and T_i are chosen based on the two temperature model, which is described later. For all of our simulations, an ultrasoft pseudopotential is used to describe the Cu ions with *3d*, *4s* and *4p* as valence states, and the electronic wavefunctions are expanded by a planewave basis with periodic boundary conditions. A cubic supercell containing 32 atoms is used. The electronic structure is optimized for each time step and the atomic configuration is propagated based on Newtonian equation.

On those atomic configurations, the x-ray absorption cross sections are calculated from the dipole transition matrix elements between the Cu *2p* core state and unoccupied states (Kohn-Sham eigenstates). The Quantum Espresso package [16] is used to generate both the atomic configurations and the Kohn-Sham eigenstates, and the prescription developed by Prendergast and Galli is used to reconstruct the oscillatory property of electronic wavefunctions near the vicinity of nuclei from the smoothed pseudo wavefunctions [17]. The k-points integration is performed using the interpolation scheme described in Ref [18]. To obtain satisfactory ensemble averages for each absorption spectrum, an average over all 32 atoms in a single cell and for 200 independent snapshots was performed. In terms of system size, the convergences of both the DOS and the absorption spectrum were achieved.

First, the XAS at the room temperature is calculated [Fig. 3(a)]. The Fermi distribution for 300 K is applied to the solid x-ray absorption cross section. The total x-ray absorption spectrum is constructed as the superposition of L_3 and L_2 edges, where the L_2 edge is obtained by shifting L_3 edge spectrum by 20 eV. The L_3:L_2 branching ratio of 1.8:1 is chosen to fit the experimental spectra. We note that deviations from the statistical 2:1 ratio of L_3:L_2 is observed for *3d* transition metals [19]. A single scaling factor adjusted the absolute cross section of all the calculations to the measurements. Energy and edge-dependent lifetime broadening is separately added to the L_3 and L_2 edge spectra [20]. The whole spectrum is convolved with a 1.1 eV Lorentzian function, representing the experimental resolution.

For warm dense matter, the x-ray absorption cross section is calculated for high temperature liquid Cu. The high temperature XAS are calculated by again applying a Fermi-Dirac distribution, because the hot electrons are expected to quickly thermalize on a timescale less than the streak camera resolution [21]. Typical comparisons of the measured and calculated

XAS are shown in the Fig 3(b,c). Because of the sensitivity of the *L*-edges to the electron temperature, the T_e can be determined with an accuracy of ~ 1000 K by comparing the edge shift and broadening. The strong red shift of the *L*-edge at early time is a consequence of the elevated electron temperature and the high *d*-DOS below the E_F. The broadening of the edge at later times (e.g. 9 ps) results from the lower electron temperatures. It is also noted that the calculated XAS reproduces the shape of the experimental XAS above the edge, which has ~ 10 % lower absorption than the room temperature solid. This reduction cannot be explained by the electron occupation at ~ 10000 K. The solid and liquid DOS at these energies are also similar [Fig 3(d)]. Therefore, the change in the XAS above the edge must be explained by a decrease in the x-ray absorption matrix elements for the *2p s, d* transitions. Overall, there is a quantitative agreement between the measured and calculated XAS.

Supplemental optical pyrometry indicates a peak brightness temperature of ~ 3100 K at 400 ps. This result is in reasonable agreement with the XAS. Density changes may result in a shift in the absorption edge [22]. However, simulations of copper at 0.5 of solid density did not well reproduce the measured XAS at and above the edges [14]. From the low density calculation and the FDI results, it is concluded that constant density is a good approximation for early time delay while at later time delay, > 5 ps, hydrodynamic expansion could play a role. We also note that the electron temperature of Cu determined by comparing experimental and calculated XAS is sensitive to the energy of the *d*-band. In fact, the calculated energy of the *d*-band of solid Cu is overestimated by 0.4 eV when referred to photoemission data. The overestimation of the *d*-band energy is a common disadvantage of the DFT methods [23].

The dynamical evolution of the electron temperature is shown in the Fig. 4. The measured T_e quickly increases to a peak of ~ 10200 K at 2 ps. It starts to decrease and reaches ~

4500 K after 10 ps. To understand the observed dynamics of warm dense copper, we employ the two-temperature model (TTM) [24]. This model, widely used for femtosecond laser-solid interactions, describes the temporal evolution of T_e and T_i according to

$$C_e(T_e)\frac{dT_e(t)}{dt} = -G(T_e)\left[T_e(t) - T_i(t)\right] + S_L(t)$$
$$C_i\frac{dT_i(t)}{dt} = G(T_e)\left[T_e(t) - T_i(t)\right]$$

Here G is the electron-phonon coupling factor, while C_e and C_i are the electron and ion heat capacities, respectively. The C_e is obtained from the derivative of the Fermi-Dirac distribution with respect to temperature. The C_i is 3.5×10^6 J/m^3 K, obtained by the Dulong-Petit law and is assumed to be constant. S_L is the energy deposition by the laser pulse. For the electron-phonon coupling parameter, a value of $G_0 = 10^{17}$ Wm^{-3} K^{-1} is experimentally measured up to the temperature of 2200 K [25]. Recently, Lin *et al*. derive an expression for the T_e-dependent electron-phonon coupling factor $G(T_e)$ and calculate the values for various metals including Cu [26], for which $G(T_e)$ increases dramatically from room temperature to a value of 5.3×10^{17} Wm^{-3} K^{-1} at 10000 K. Using the calculated $C_e(T_e)$ and the values of $G(T_e)$ from the Ref. [26], $T_e(t)$ and $T_i(t)$ have been derived. The same calculations with a constant $G_0 = 10^{17}$ Wm^{-3} K^{-1} have also been performed for comparison. The results are shown in Fig. 4.

Both results show that the electron temperature peaks at the end of the laser pulse, and then decreases. But comparing to the constant G_0, the temperature dependent $G(T_e)$ provides lower values of T_e, a faster decrease in T_e, and as a result a better agreement with the experimental data. It indicates that the electron-phonon coupling factor of Cu is enhanced in this temperature regime. We note that at longer time delay the experimentally-observed electron temperatures are lower than the TTM calculations, indicating the onset of additional electron cooling mechanisms. Hydrodynamic motion is a possible cause.

In conclusion, we have observed the evolution of the unoccupied electron DOS of warm dense copper via time-resolved XAS. Good agreement is observed between measured XAS and calculated spectra based on the DOS of liquid Cu. From the edge shift and broadening, the electron temperature of non-equilibrium states of warm dense matter could be determined in the 10000 K regime. The reduction of x-ray absorption above the edge results from a change in the transition matrix elements. The evolution of electron temperature can be described by a two-temperature model including T_e-dependent electron heat capacities and electron-phonon coupling factors.

The authors would like to acknowledge stimulating discussions with E. Henestroza, A. Ng and J. Cao. These experiments were carried out at the ALS, supported by the Director, Office of Science, Office of Basic Energy Sciences, Materials Sciences Division, of the U.S. Department of Energy under Contract No. DEAC03-76SF00098 at LBNL and a part of the work was performed by LLNL under Contract DEAC52-07NA27344 and the LDRD program at LLNL (08-ERD-005).

References

[1] Y. Ping *et al.*, Physical Review Letters **96**, 255003 (2006).

[2] A. Nelson *et al.*, Applied Physics Letters **87**, 154102 (2005).

[3] H. J. Lee *et al.*, Physical Review Letters **102**, 115001 (2009).

[4] A. Mančić *et al.*, Physical Review Letters **104**, 35002 (2010).

[5] R. W. Lee *et al.*, Laser and Particle Beams **20**, 527 (2002).

[6] M. Ross, Nature **292**, 435 (1981).

[7] M. Koenig *et al.*, Applied Physics Letters **72**, 1033 (1998).

[8] J. Chan *et al.*, Optics Letters **26**, 1726 (2001).

[9] P. Ni *et al.*, Laser and Particle Beams **26**, 583 (2008).

[10] S. Johnson *et al.*, Physical Review Letters **91** (2003).

[11] P. Heimann *et al.*, AIP Conference Proceedings **879**, 1195 (2007).

[12] J. Feng *et al.*, Applied Physics Letters **96**, 134102 (2010).

[13] J. Hohlfeld *et al.*, Chemical Physics **251**, 237 (2000).

[14] FDI measurments and variable density XAS calculationswill be presented separately.

[15] M. Grioni *et al.*, Physical Review B **39**, 1541 (1989).

[16] Paolo Giannozzi et al., Journal of Physics: Condensed Matter **21**, 395502 (2009).

[17] D. Prendergast, and G. Galli, Physical Review Letters **96**, 215502 (2006).

[18] D. Prendergast, and S. G. Louie, Physical Review B **80**, 235126 (2009).

[19] R. D. Leapman, and L. A. Grunes, Physical Review Letters **45**, 397 (1980).

[20] J. E. Müller, O. Jepsen, and J. W. Wilkins, Solid State Communications **42**, 365 (1982).

[21] W. S. Fann *et al.*, Physical Review Letters **68**, 2834 (1992).

[22] V. Recoules, and S. Mazevet, Physical Review B **80**, 064110 (2009).

[23] V. P. Zhukov, and E. V. Chulkov, Physics Uspekhi **52**, 105 (2009).

[24] S. Anisimov, B. Kapeliovich, and T. Perel'man, Sov. Phys. JETP **39**, 375 (1974).

[25] H. Elsayed-Ali *et al.*, Physical Review Letters **58**, 1212 (1987).

[26] Z. Lin, L. Zhigilei, and V. Celli, Physical Review B **77**, 075133 (2008).

Figures & Captions

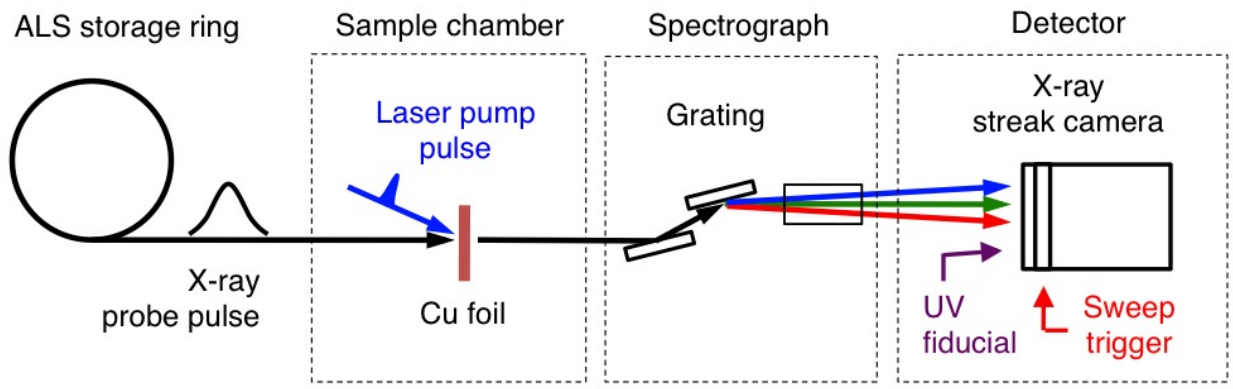

Fig 1. Schematic diagram of the experiment.

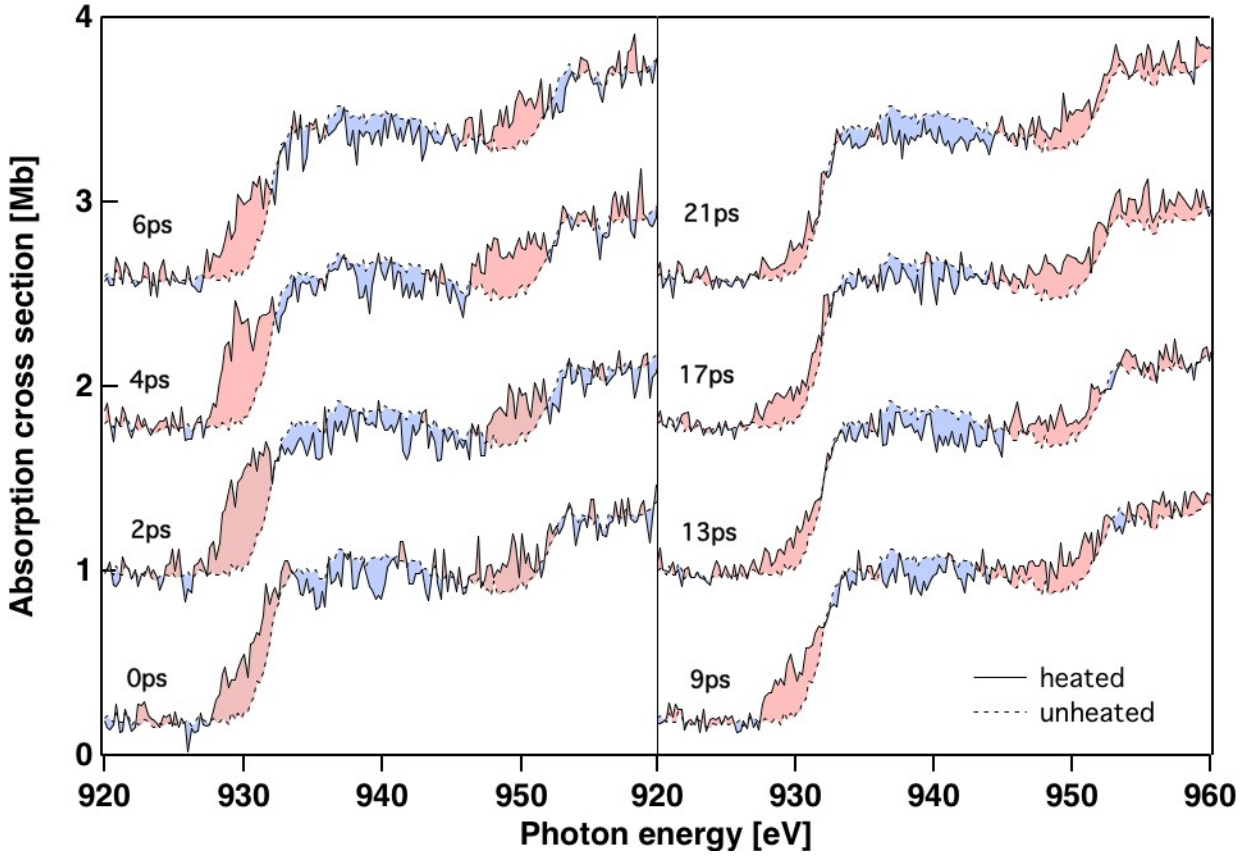

Fig 2. The XAS of warm dense copper at selected times (solid curves). Spectra are displayed with an offset of +0.8 along the *y*-axis between time steps. For comparison, the room temperature XAS of Cu is also shown as the dotted curves.

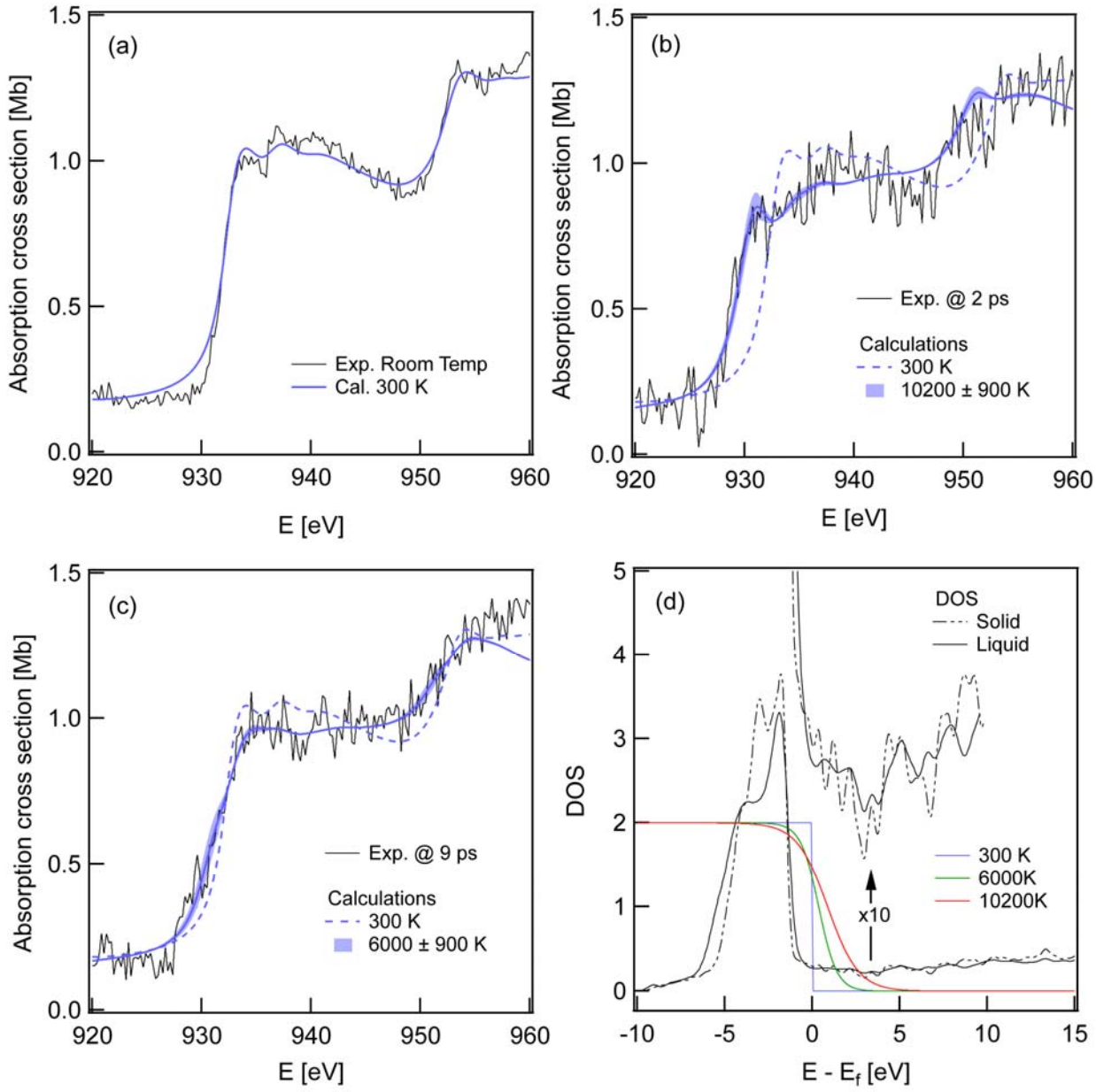

Fig 3. Comparisons of measured and calculated XAS for (a) the ambient and (b,c) the WDM states of Cu at selected times. Experimental data are shown as black curves and calculations at the given temperatures as blue curves. (d) The DOS of solid (dotted line) and liquid (solid line) Cu and the electron distributions at the temperatures used in the modeling.

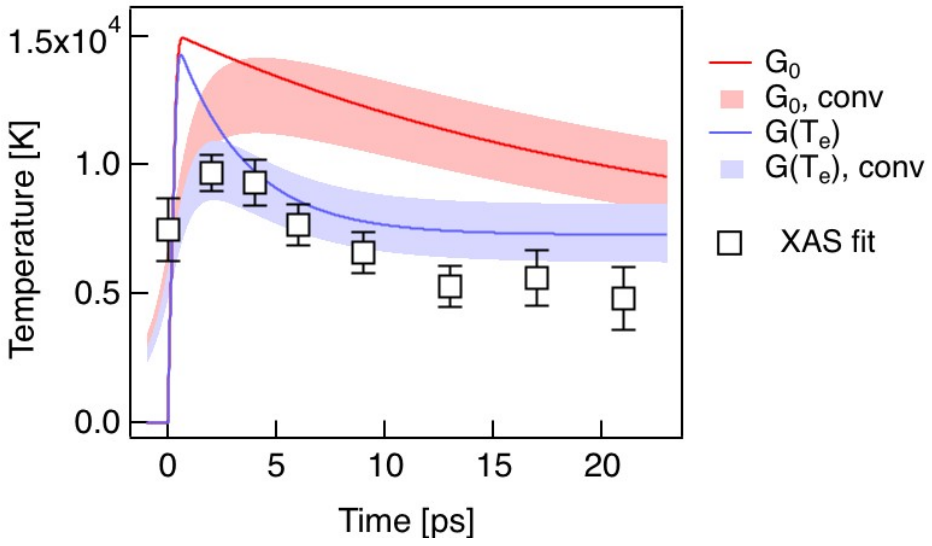

Fig 4. The temporal evolution of the T_e. Experimental-derived values of the T_e are shown as squares. For G_0 (red) and $G(T_e)$ (blue), solid lines are the T_e calculated by the TTM. The shaded curves include the experimental accuracies in the E_d and the temporal resolution of the detector.